J. Biochem. **143,** 617–623 (2008)
doi:10.1093/jb/mvn012

Characterization of Dihydrodipicolinate Reductase from *Thermotoga maritima* Reveals Evolution of Substrate Binding Kinetics

F. Grant Pearce*, Clara Sprissler and Juliet A. Gerrard
School of Biological Sciences, University of Canterbury, Private Bag 4800, Christchurch 8020, New Zealand

Received January 6, 2008; accepted January 16, 2008; published online February 4, 2008

In lysine biosynthesis, dihydrodipicolinate reductase (DHDPR) catalyses the formation of tetrahydrodipicolinate. Unlike DHDPR enzymes from *Escherichia coli* and *Mycobacterium tuberculosis*, which have dual specificity for both NADH and NADPH as co-factors, the enzyme from *Thermotoga maritima* has a significantly greater affinity for NADPH. Despite low sequence identity with the *E. coli* and *M. tuberculosis* DHDPR enzymes, DHDPR from *T. maritima* has a similar catalytic site, with many conserved residues involved in interactions with substrates. This suggests that as the enzyme evolved, the co-factor specificity was relaxed. Kinetic studies show that the *T. maritima* DHDPR enzyme is inhibited by high concentrations of its substrate, DHDP, and that at high concentrations NADH also acts as an inhibitor of the enzyme, suggesting a novel method of regulation for the lysine biosynthetic pathway. Increased thermal stability of the *T. maritima* DHDPR enzyme may be associated with the lack of C-terminal and N-terminal loops that are present in the *E. coli* DHDPR enzyme.

Key words: dihydrodipicolinate reductase, lysine biosynthesis, pyridine nucleotide specificity, thermophilic enzymes, *Thermotoga maritima*.

Abbreviations: (S)-ASA, (S)-aspartate-β-semialdehyde; DHDPR, dihydrodipicolinate reductase; DHDP-synthase, dihydrodipicolinate synthase; DHDP, dihydrodipicolinate; PDC, 2,6-pyridinedicarboxylate.

Lysine is an essential amino acid and, as such, inhibition of the lysine biosynthetic pathway may lead to the development of novel antibiotics and pesticides (*1*,*2*). In bacteria, three routes are known for the biosynthesis of lysine via diaminopimelate, which is an essential component of the peptidoglycan layer of cell walls in both Gram positive and Gram negative bacteria. (S)-Tetrahydrodipicolinate is a precursor for each of the three bacterial lysine biosynthetic pathways, and is the product of dihydrodipicolinate reductase (DHDPR). DHDPR was first purified from *Escherichia coli* (*3*), and has been shown to catalyse the NAD(P)H-dependent reduction of an unstable heterocyclic substrate, dihydrodipicolinate (DHDP) (*4*, *5*).

DHDPR from *E. coli* (a gamma proteobacterium) and *Mycobacterium tuberculosis* (an actinobacterium) have been well characterized (*4*, *6*, *7*), and the X-ray crystal structures have been solved for these species (*7–9*). Recently, the structural coordinates for *Thermotoga maritima* DHDPR have been deposited in the PDB (1vm6). *Thermotoga maritima* is a thermophilic, Gram-negative bacterium, and small-subunit ribosomal RNA phylogeny has placed this bacterium as one of the deepest and most slowly evolving lineages in the bacteria (*10*). Phylogenetic analysis of genes encoding DHDPR has previously shown several major clusters that align well with phylogenetic lineages deduced from 16S ribosomal RNA genes (*11*). Among these clusters, *T. maritima* is distinct from other groups, as are gamma proteobacteria and actinobacteria.

While most pyridine nucleotide-dependent dehydrogenase enzymes have a strong preference for either 2′-phosphorylated (NADPH) or non-phosphorylated (NADH) nucleotide substrates (*6*), *E. coli* DHDPR enzyme is unusual in that it has similar specificity for both pyridine nucleotides (*1*, *4*). *Mycobacterium tuberculosis* DHDPR also has similar specificity for both pyridine nucleotides, and mutations have been shown to alter the nucleotide specificity (*7*). *Escherichia coli* DHDPR is competitively inhibited by 2,6-pyridinedicarboxylate (PDC), an aromatic analogue of dihydrodipicolinate, and also by $NADP^+$ (*4*). Inhibitors have also been designed that target *M. tuberculosis* DHDPR (*12*), and it has recently been reported that DHDPR from the methylotroph *Methylophilus methylotrophus* is inhibited by lysine (*13*).

As part of our investigations into the enzymes involved in lysine biosynthesis, and following the characterization of dihydrodipicolinate synthase (DHDP-synthase) from *T. maritima* (*14*), the activity of *T. maritima* DHDPR has been studied. These results, combined with an analysis of known enzyme structures and sequences, provide an increased knowledge of how different DHDPR enzymes utilize pyridine nucleotides and provide insights into how the selection of co-factors evolved.

*To whom correspondence should be addressed. Tel: +64 3 364 2987; Fax: +64 3 364 2590,
E-mail: grant.pearce@canterbury.ac.nz

EXPERIMENTAL PROCEDURES

Materials—Unless otherwise stated, all chemicals were obtained from Sigma Chemical Co., GE Biosciences or Invitrogen. Protein concentration was measured by the method of Bradford (*15*). Unless otherwise stated, enzymes were manipulated at 4°C or on ice. (S)-ASA [(S)-aspartate-β-semialdehyde] was synthesized using the method of Roberts (*16*) and was of high quality (>95%) as judged by ^{1}H NMR and the coupled assay. DHDP-synthase from *T. maritima* was purified by previously reported methods (*14*).

Cloning, Over-expression and Purification—Primer pairs encoding the predicted 5′ and 3′ ends of the TM1520 open reading frame (*17*) were used to amplify the *dap*B gene from *T. maritima* strain MSB8 genomic DNA. The PCR product included a purification tag (MGSDKIHHHHHH) at the amino terminus of the full length protein, and was cloned into the pMH1 plasmid, which was a kind donation from Scott Lesley and Heath Klock (Joint Center for Structural Genomics, Genomics Institute of the Novartis Research Foundation, San Diego) and introduced to the *E. coli* XL-1 Blue strain. Protein expression from *E. coli* XL-1 Blue cells was performed in LB media, and culture were grown overnight at 37°C. Protein expression was induced by the addition of 0.15% arabinose, and cells were incubated for a further 3 h. The cells were harvested by centrifugation (10 min, 4,000*g*, 4°C) and resuspended in two volumes of extraction buffer (50 mM NaH_2PO_4, pH 8.0, 20 mM imidazole, 300 mM NaCl). After lysis by sonication, cell debris was pelleted by centrifugation at 13,000*g* for 10 min, and the supernatant was applied to a His-Trap column (GE Biosciences). The column was washed with extraction buffer for three column volumes, and then protein was eluted with elution buffer (50 mM NaH_2PO_4, pH 8.0, 300 mM imidazole, 300 mM NaCl). Fractions containing DHDPR activity were pooled, dialysed against storage buffer (20 mM Tris–HCl, pH 8.0) and stored at −20°C.

Thermal Stability—Thermal shift assays were carried out as described previously (*18*). A total of 25 μl of solution containing 0.5 mg/ml protein and 10× Sypro Orange dye (Invitrogen) were added to the wells of a 96-well thin-wall PCR plate (Bio-Rad). NADH or NADPH (150 μM) were added to some samples. The plates were sealed and heated in an iCycler iQ Real Time PCR Detection System (Bio-Rad) from 40°C to 100°C in increments of 0.2°C, with 10 s dwell time. Fluorescence changes in the wells of the plate were monitored simultaneously with a charge-coupled device (CCD) camera. The wavelengths for excitation and emission were 490 and 575 nm, respectively. Experiments were carried out in triplicate for each condition, and the temperature midpoint (T_m) determined by using a Boltzmann model, as previously described (*18*).

Enzyme Kinetics—DHDPR activity was measured using a coupled assay with DHDP-synthase to form the substrate, as previously described (*1*). Stock solutions of (*S*)-ASA, NADPH, NADH and pyruvate were prepared fresh for each experiment, and the cuvettes were incubated for 60 s with an excess of DHDP-synthase (20–100 μg/ml) before the assays were initiated by the addition of DHDPR. Assay temperature was regulated by the use of a circulating water bath, and assays were performed at 30°C or 45°C. The amount of DHDPR in the assays was typically 0.2–100 μg/ml. Initial rate data were usually reproducible within 10%, and were analysed using non-linear regression software (OriginLab, Northampton, MA, USA) or the program Enzfitter (Biosoft, Cambridge, UK). Equation (1) was used for fitting substrate inhibition by DHDP, Equation (2) for fitting Michaelis–Menten constants for NADPH and NADH, and Equation (3) for inhibition by NADH:

$$v = \frac{V^{(app)}[A]}{(K_m^{(app)}) + [A] + [A]^2/K_{iS})} \quad (1)$$

$$v = \frac{V^{(app)}[A]}{(K_m^{(app)}) + [A])} \quad (2)$$

$$v = \frac{V^{(app)}}{(1 + [I]/K_i)} \quad (3)$$

Here, the unknown constants include the apparent maximal velocity ($V^{(app)}$), apparent Michaelis–Menten constant ($K_m^{(app)}$), substrate inhibition constant (K_{iS}) and inhibition constant (K_i), while the known variables include the substrate concentration ([A]), inhibitor concentration ([I]) and the initial velocity (v) (*19*). It was not possible to obtain kinetic parameters at thermophilic temperatures, due to the inherent instability of the substrate, (*S*)-ASA at these temperatures (*20*).

RESULTS AND DISCUSSION

Structural Studies of T. maritima DHDPR—Structural coordinates for *T. maritima* DHDPR complexed with the NADH co-factor have recently been deposited in the protein databank (1vm6). Comparison of the *E. coli*, *M. tuberculosis* and *T. maritima* DHDPR enzymes reveal that, despite a low sequence identity (38%), the enzymes have a very similar homotetrameric structure (Fig. 1). The monomer consists of two domains, an N-terminal domain, which is a dinucleotide binding fold, and a C-terminal domain, which is the DHDP and PDC inhibitor binding domain (*7*, *8*). Despite the conserved structure, there are several differences between the different enzymes. It has previously been reported that the enzyme from *M. tuberculosis* lacks a 22 amino acid loop in the N-terminal domain that is present in the *E. coli* enzyme, and that the direction of a long loop in the C-terminal domain is different between the two enzymes (*7*). Examination of the *T. maritima* DHDPR structure reveals that this enzyme lacks the N-terminal domain loop and also lacks the long loop in the C-terminal domain.

Structures of *E. coli* and *M. tuberculosis* DHDPR enzymes complexed with NADPH or NADH, and also with the inhibitor PDC, which is an analogue of the DHDP substrate, have previously been solved (*6–9*). Comparison of these structures shows that when PDC and a co-factor are bound in the active site, there is a closure of the monomeric subunit, which involves a 10° rotation of the C-terminal domain relative to the N-terminal domain around a hinge region (*6*). The *E. coli* DHDPR structure (1arz) shows three

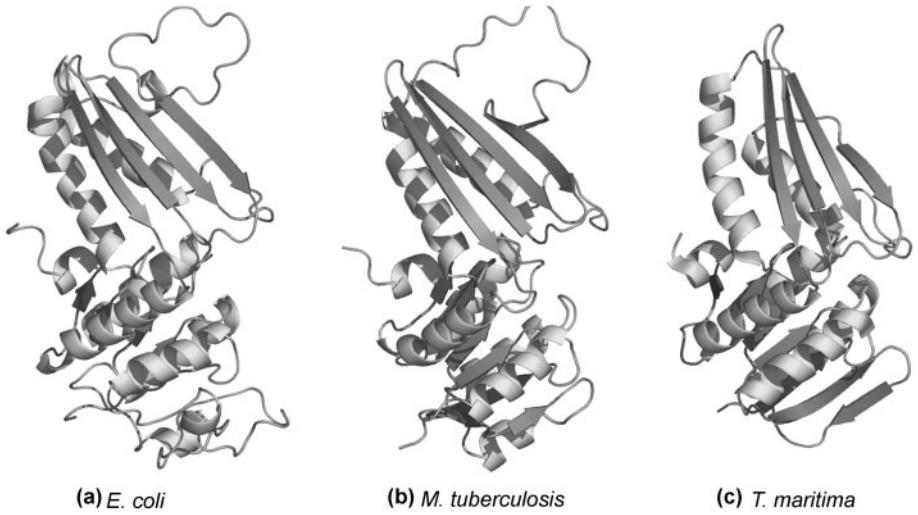

Fig. 1. **Comparison of the DHDPR monomers for (A) *E. coli* (1arz), (B) *M. tuberculosis* (1c3v) and (C) *T. maritima* (1vm6).** The C-terminal loop is seen on the upper right of the *E. coli* and *M. tuberculosis* monomers, but is lacking in the *T. maritima* monomer. The N-terminal loop is seen on the lower right of the *E. coli* monomer, but is lacking in the *M. tuberculosis* and *T. maritima* monomers. Figure produced using PyMOL (*30*).

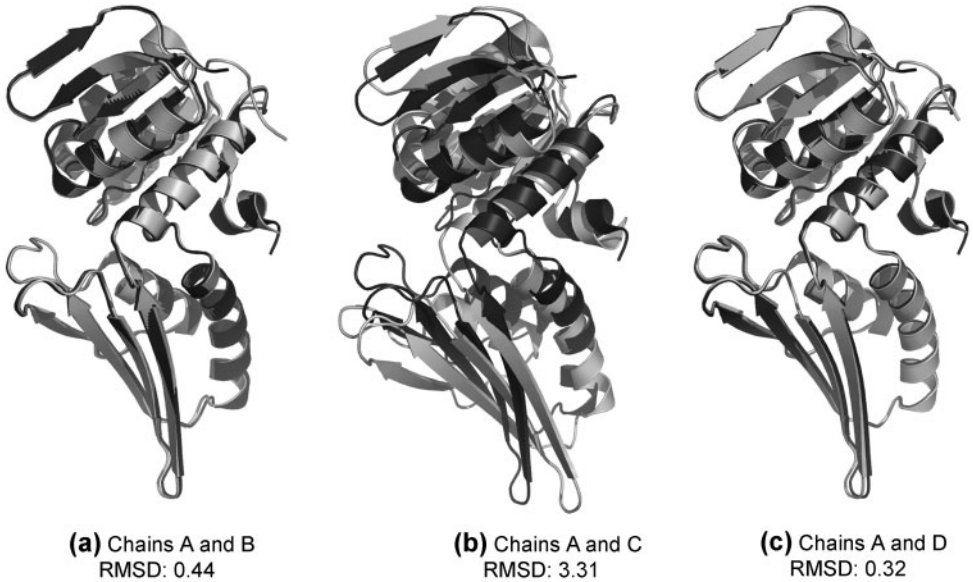

Fig. 2. **RMS differences for Cα positions (in Å) between monomers in the 1vm6 structure of *T. maritima* DHDPR show that while chains A, B and D are in a similar, closed conformation, chain C is in a more open conformation.** Monomer alignments were carried out, and structures drawn using PyMOL (*30*).

subunits in the closed conformation with both PDC and NADH bound, while the remaining subunit has only NADH bound and is in the open conformation.

Analysis of the *T. maritima* DHDPR structure shows that NADH is bound to all four of the monomers. Alignment of the four chains of the *T. maritima* DHDPR structure shows that three of the subunits (chains A, B and D) are in a nearly identical, closed conformation, while the remaining subunit (chain C) is in the open conformation (Fig. 2). The three subunits of *T. maritima* DHDPR that are in the closed conformation have acetate bound at the position occupied by PDC in the *E. coli* and *M. tuberculosis* structures, with chain A and chain B containing two acetate molecules, while chain D contains only one.

Previous analysis of the structures suggested that the unusual dual specificity of *E. coli* DHDPR was due to an acidic residue, Glu-38, interacting with the ribose 2′ and 3′ hydroxyl groups of NADH, while an adjacent basic residue, Arg-39, interacts with the 2′-phosphate of NADPH (*6*). The acidic residue is conserved in *M. tuberculosis* DHDPR, with Asp-33 forming hydrogen bonds with the ribose 2′ and 3′ hydroxyl groups of NADH, while the basic residues Lys-9 and Lys-11 interact with the phosphate group of NADPH (*7*). *T. maritima* DHDPR also has an equivalent acidic residue, in the form of Asp-32, although

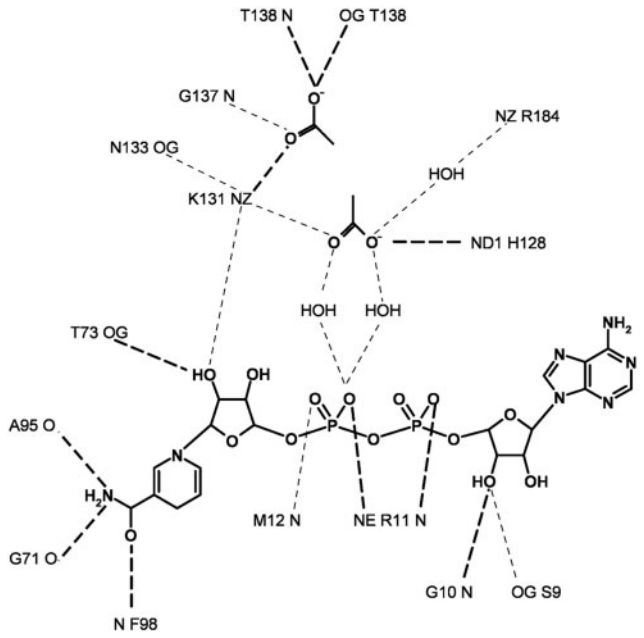

Fig. 3. **Schematic diagram of the binding sites for NADH and acetate molecules in the closed chains (A and B) of the *T. maritima* structure (1vm6).** Hydrogen bonds are indicated by dashed lines. Bonds that are conserved between the *T. maritima*, *E. coli* and *M. tuberculosis* enzymes are shown in bold. Residue numbering is shown for the *T. maritima* enzyme.

there do not appear to be any interactions between this residue and the ribose hydroxyl groups of NADH. It is likely that the nearby basic residues of Lys-132 and/or Arg-11 interact with the 2′-phosphate group of NADPH. Many of the other interactions between NADH and other residues of the *T. maritima* DHDPR monomer are conserved when compared to the *E. coli* and *M. tuberculosis* enzyme structures.

Numerous hydrogen bonds are also conserved in the DHDP/PDC binding site, with the two acetate molecules in chains A and B forming hydrogen bonds with Lys-131, Gly-137, Thr-138, and His-128 (Fig. 3). This region is located in a region of the C-terminal domain that is highly conserved (*8*). It appears that the binding of acetate in the DHDP/PDC binding site is sufficient to trigger closure of the monomeric subunit.

Thermal Stability of T. maritima DHDPR—Increased thermal stability has previously been observed for the *T. maritima* DHDP-synthase enzyme (*14*), and it is thought that thermostability of enzymes is due to increased electrostatic interactions and compactness (*21*, *22*). Differential scanning fluorimetry is a technique that measures the thermal unfolding of proteins in the presence of a fluorescent dye (*18*). Thermal analysis of the DHDPR enzymes by differential scanning fluorimetry showed that in the absence of ligand, *E. coli* DHDPR had a T_m of 69.5°C, while *T. maritima* DHDPR had a T_m at 95.7°C (Fig. 4). This is in agreement with kinetic studies showing that incubation of the *E. coli* enzyme at 80°C resulted in a lack of activity within a few minutes, while the *T. maritima* enzyme was stable for up to 48 h (data not shown). It is likely that the absence of the C-terminal and N-terminal loops of *T. maritima* DHDPR is related

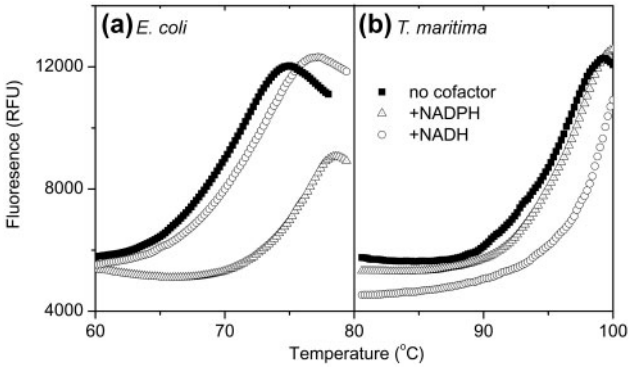

Fig. 4. **Thermal shift assay results for *E. coli* (a) and *T. maritima* (b) DHDPR in the absence (squares) of co-factor, or in the presence of 150 μM NADH (circles) or NADPH (triangles).**

to the higher thermostability. Previous studies of the triosephosphate isomerase enzyme have shown that the thermophilic form of the enzyme is much more compact than the mesophilic form, with pruning of several helices and truncation of loops (*23*).

Thermal scanning can also be used to detect ligand binding through ligand-induced stabilization of proteins (*24*). Addition of the NADH co-factor increased the T_m of the *T. maritima* enzyme by >5°C, while NADPH had less of an effect (ΔT_m of 1.6°C) (Fig. 4). Conversely, NADPH increased the stability of the *E. coli* DHDPR enzyme (ΔT_m of 5.8°C) more than the NADH co-factor (ΔT_m of 1.8°C). These results suggest that there are differences in nucleotide specificity and binding between the two DHDPR enzymes.

Enzyme Kinetics with Respect to DHDP and NAD(P)H—To determine the co-factor specificity of *T. maritima* DHDPR, assays were carried out by varying the concentration of NADH or NADPH, but maintaining a fixed (50 μM) concentration of DHDP. This showed that the maximal enzyme rate using NADH as a co-factor is 3% of the maximal enzyme rate using NADPH as a co-factor, which is in contrast to the previous characterization of DHDPR from *E. coli* (*4*) and *M. tuberculosis* (*7*), which has dual specificity, with similar rates using either NADH or NADPH as a co-factor. The $K_m^{(app)}$ for NADPH and NADH were measured to be 0.6 ± 0.1 and 2.5 ± 0.3 μM, respectively at 30°C (Table 1), which are similar to the previously determined Michaelis–Menten constants for *E. coli* (*4*) and *M. tuberculosis* (*7*) DHDPR. When the kinetic parameters were measured at 45°C instead of 30°C, there was an increase in the specificity constant ($k_{cat}^{(app)}/K_m^{(app)}$) for both substrates (Table 1). This was mostly due to an increase in the catalytic rate, which was consistent with the temperature dependence of chemical reactions.

When *T. maritima* DHDPR was assayed with constant concentrations of NADH or NADPH, and varying concentrations of DHDP, it was apparent that the enzyme was inhibited by increased concentrations of the DHDP substrate (Fig. 5, Table 1), which has not been observed for *E. coli* or *M. tuberculosis* DHDPR. Like the assays carried out to determine the kinetic parameters for DHDP, these assays showed a slower reaction rate

Table 1. **Kinetic parameters (±SD) for *T. maritima* DHDPR were calculated as described in the Experimental methods section.**

	NADPH (constant DHDP)		NADH (constant DHDP)		DHDP (constant NADPH)	
	30°C	45°C	30°C	45°C	30°C	45°C
$k_{cat}^{(app)}$ (s^{-1})	2.6 ± 0.1	17 ± 1	0.093 ± 0.003	0.49 ± 0.03	8.1 ± 1.3	19 ± 2
$K_m^{(app)}$ (μM)	0.6 ± 0.1	2.1 ± 0.5	2.5 ± 0.3	1.8 ± 0.5	7.6 ± 2.3	13 ± 3
$K_{cat}^{(app)}/K_m^{(app)}$ (s^{-1}/μM)	4.3 ± 0.9	8.1 ± 0.3	0.037 ± 0.006	0.27 ± 0.09	1.1 ± 0.5	1.5 ± 0.5
K_{iS} (μM)	–	–	–	–	27 ± 7	152 ± 45

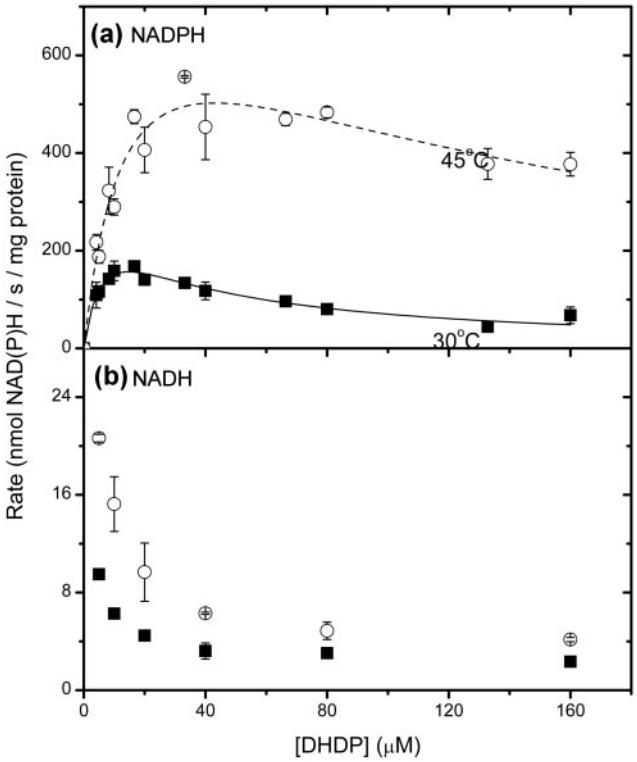

Fig. 5. **Kinetics of *T. maritima* DHDPR with respect to DHDP.** Assays were carried out at fixed (160 μM) NADPH (panel a) or NADH (panel b) concentration and varying DHDP concentrations at 30°C (squares) and 45°C (circles). Initial rate data for NADPH were fitted to a model describing substrate inhibition. Absence of data at low concentrations of DHDP precluded modelling of initial rate data for NADH. Each data point was measured in duplicate or triplicate, and error bars show the standard deviation. Data were fitted to an equation describing substrate inhibition (Equation 1) and the parameters determined are shown in Table 1.

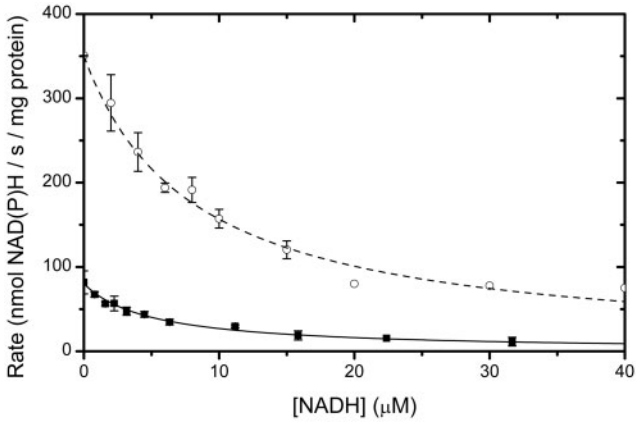

Fig. 6. **Kinetics of *T. maritima* DHDPR at fixed NADPH (160 μM) and DHDP (50 μM) concentrations with varying NADH concentrations at 30°C (squares) and 45°C (circles).** Initial rate data were fitted to a model describing inhibition. Each data point was measured in duplicate or triplicate, and error bars show the standard deviation.

with the NADH co-factor than the NADPH cofactor (Fig. 5). While kinetic parameters could be determined for DHDPR using NADPH as a co-factor, kinetic parameters were not able to be calculated for DHDPR using NADH as a co-factor, due to increasing amounts of error in measuring the reaction rate at low substrate concentrations. Monitoring the progress of the reaction over time showed that the highest reaction rates occurred at around 5 μM DHDP (data not shown).

As seen in the assays carried out to determine the kinetic constants with respect to NAD(P)H, there was an increase in catalytic rate at the higher temperature of 45°C (Fig. 5, Table 1), which was consistent with the Arrhenius temperature dependence of enzyme activity. Higher temperatures also reduced the effect of substrate inhibition, with a 5-fold increase in the K_{iS} constant (Table 1). This change in inhibition pattern may be due to reduced flexibility at lower temperatures. Studies of enzyme dynamics have shown that at any given temperature, thermostable enzymes, such as those from *T. maritima*, have reduced flexibility compared with thermolabile ones (*25*). If *T. maritima* DHDPR has reduced flexibility at 30°C, relative to 45°C, there may be an increased likelihood of DHDP binding to form an inactive complex at lower temperatures. Substrate inhibition by DHDP is unlikely to be physiologically relevant, as tight control of metabolism would normally couple the production of DHDP by DHDP-synthase with consumption by DHDPR, preventing an accumulation of DHDP *in vivo*. Previous studies have suggested that at lower temperatures, enzymes from extreme thermophiles are often less active than those from mesophiles (*26*, *27*). However, despite being assayed at a temperature well below the optimum growth temperature of 80°C (*28*), the *T. maritima* DHDPR activity was similar to that of the mesophilic *E. coli* enzyme (*1*).

Inhibition of T. maritima DHDPR by NADH— Following the observation that *T. maritima* DHDPR does not utilize NADH as a co-factor, the role of NADH in inhibiting the enzyme was examined. Initial rate assays of *T. maritima* DHDPR at high concentrations of DHDP and NADPH showed inhibition by NADH (Fig. 6).

At 30°C and 45°C, NADH had a K_i of 5.1 ± 0.6 and 8.1 ± 0.6 μM, respectively.

In plants and most Gram-negative bacteria, regulation of lysine and diaminopimelate biosynthesis is carried out by the feedback inhibition of the DHDP-synthase or aspartate kinase enzyme by lysine. Analysis of the *T. maritima* DHDP-synthase enzyme (*14*) showed a lack of inhibition by lysine, and it has been postulated that lysine biosynthesis in *T. maritima* is regulated by aspartate kinase or at the level of gene regulation (*29*). While other studies have suggested that some DHDPR enzymes are directly inhibited by lysine (*13*), there was no evidence for inhibition of *T. maritima* DHDPR by lysine (data not shown). The results in this study suggest that regulation of lysine biosynthesis in *T. maritima* may involve the inhibition of DHDPR by NADH.

CONCLUSIONS

High thermal stability is required for DHDPR to function at 80°C, the optimum growth temperature of *T. maritima* (*28*). The C-terminal loop has been proposed to stabilize the *E. coli* and *M. tuberculosis* tetramers by wrapping around the central β-sheet (*7*), but the absence of this loop in the *T. maritima* DHDPR enzyme suggests that thermal stability is due to other factors, such as increased electrostatic interactions (*21*, *22*). Thermal shift assays confirmed the high thermal stability of the *T. maritima* enzyme, and also showed differences in ligand binding for the NADH and NADPH co-factors.

Unlike DHDPR enzymes previously characterized from *E. coli* and *M. tuberculosis*, *T. maritima* DHDPR does not show dual pyridine nucleotide specificity, instead showing increased affinity for NADPH. *Thermotoga maritima* is one of the deepest and most slowly evolving Eubacterial lineages (*10*), and may provide the closest relative of ancestral DHDPR enzymes. It is thus likely that the nucleotide requirements of the DHDPR enzyme has been relaxed during evolution, leading to the use of NADH as a co-factor by the *E. coli* and *M. tuberculosis* DHDPR enzymes.

One consequence of the lack of availability of NADH as a co-factor by *T. maritima* DHDPR is that the nucleotide can act to regulate lysine and diaminopimelate biosynthesis. Structural studies have shown that NADH can bind to the *T. maritima* enzyme and trigger a change from the open to the closed conformation, even in the absence of the second substrate. It is likely that this tight complex is responsible for the increased thermal stability in the presence of NADH. Unlike plants and other Gram-negative bacteria, *T. maritima* DHDP-synthase is not feedback regulated by lysine (*14*), and the inhibition of *T. maritima* DHDPR by NADH may provide mechanisms for regulation of lysine biosynthesis in this bacterium.

FUNDING

We thank Drs Scott Lesley and Heath Klock, Joint Centre for Structural Genomics, Genomics Institute of the Novartis Research Foundation, San Diego, for supplying the plasmid and for useful discussion and comment and Jackie Healy for zealous technical support. This work was funded, in part, by the Royal Society of New Zealand, Marsden Fund and, in part, by the Foundation of Research, Science and Technology via a fellowship to F.G.P.

REFERENCES

1. Coulter, C.V., Gerrard, J.A., Kraunsoe, J.A.E., and Pratt, A.J. (1999) *Escherichia coli* dihydrodipicolinate synthase and dihydrodipicolinate reductase: kinetic and inhibition studies of two putative herbicide targets. *Pesticide Sci.* **55**, 887–895
2. Cox, R., Sutherland, A., and Vederas, J. (2000) Bacterial diaminopimelate metabolism as a target for antibiotic design. *Bioorg. Med. Chem.* **8**, 843–871
3. Tamir, H. and Gilvarg, C. (1974) Dihydrodipicolinic acid reductase. *J. Biol. Chem.* **249**, 3034–3040
4. Reddy, S.G., Sacchettini, J.C., and Blanchard, J.S. (1995) Expression, purification, and characterization of *Escherichia coli* dihydrodipicolinate reductase. *Biochemistry* **34**, 3492–3501
5. Blickling, S., Renner, C., Laber, B., Pohlenz, H., Holak, T., and Huber, R. (1997) Reaction mechanism of *Escherichia coli* dihydrodipicolinate synthase investigated by X-ray crystallography and NMR spectroscopy. *Biochemistry* **36**, 24–33
6. Reddy, S.G., Scapin, G., and Blanchard, J.S. (1996) Interaction of pyridine nucleotide substrates with *Escherichia coli* dihydrodipicolinate reductase: thermodynamic and structural analysis of binary complexes. *Biochemistry* **35**, 13294–13302
7. Cirilli, M., Zheng, R., Scapin, G., and Blanchard, J.S. (2003) The three-dimensional structures of the *Mycobacterium tuberculosis* dihydrodipicolinate reductase-NADH-2,6-PDC and -NADPH-2,6-PDC complexes. Structural and mutagenic analysis of relaxed nucleotide specificity. *Biochemistry* **42**, 10644–10650
8. Scapin, G., Reddy, S.G., Zheng, R., and Blanchard, J.S. (1997) Three-dimensional structure of *Escherichia coli* dihydrodipicolinate reductase in complex with NADH and the inhibitor 2,6-pyridinedicarboxylate. *Biochemistry* **36**, 15081–15088
9. Scapin, G., Blanchard, J.S., and Sacchettini, J.C. (1995) Three-dimensional structure of *Escherichia coli* dihydrodipicolinate reductase. *Biochemistry* **34**, 3502–3512
10. Achenbach-Richter, L., Gupta, R., Stetter, K.O., and Woese, C.R. (1989) Were the original Eubacteria thermophiles? *Syst. Appl. Microbiol.* **9**, 34–39
11. Hudson, A.O., Bless, C., Macedo, P., Chatterjee, S.P., Singh, B.K., Gilvarg, C., and Leustek, T. (2005) Biosynthesis of lysine in plants: evidence for a variant of the known bacterial pathways. *Biochim. Biophys. Acta* **1721**, 27–36
12. Paiva, A.M., Vanderwall, D.E., Blanchard, J.S., Kozarich, J.W., Williamson, J.M., and Kelly, T.M. (2001) Inhibitors of dihydrodipicolinate reductase, a key enzyme of the diaminopimelate pathway of *Mycobacterium tuberculosis*. *Biochim Biophys Acta* **1545**, 67–77
13. Tsujimoto, N., Gunji, Y., Ogawa-Miyata, Y., Shimaoka, M., and Yasueda, H. (2006) L-Lysine biosynthetic pathway of *Methylophilus methylotrophus* and construction of an L-lysine producer. *J. Biotechnol.* **124**, 327–337
14. Pearce, F.G., Perugini, M.A., McKerchar, H.J., and Gerrard, J.A. (2006) Dihydrodipicolinate synthase from *Thermotoga maritima*. *Biochem. J.* **400**, 359–366
15. Bradford, M. (1976) A rapid and sensitive method for the quantitation of microgram quantities of protein utilizing the principle of protein-dye binding. *Anal. Biochem.* **72**, 248
16. Roberts, S.J., Morris, J.C., Dobson, R.C.J., and Gerrard, J.A. (2003) The preparation of (*S*)-aspartate semi-aldehyde

appropriate for use in biochemical studies. *Bioorg. Med. Chem. Lett.* **13**, 265–267
17. Nelson, K.E., Clayton, R.A., Gill, S.R., Gwinn, M.L., Dodson, R.J., Haft, D.H., Hickey, E.K., Peterson, J.D., Nelson, W.C., Ketchum, K.A., McDonald, L., Utterback, T.R., Malek, J.A., Linher, K.D., Garrett, M.M., Stewart, A.M., Cotton, M.D., Pratt, M.S., Phillips, C.A., Richardson, D., Heidelberg, J., Sutton, G.G., Fleischmann, R.D., Eisen, J.A., White, O., Salzberg, S.L., Smith, H.O., Venter, J.C., and Fraser, C.M. (1999) Evidence for lateral gene transfer between Archaea and Bacteria from genome sequence of *Thermotoga maritima*. *Nature* **399**, 323–329
18. Ericsson, U.B., Hallberg, B.M., DeTitta, G.T., Dekker, N., and Nordlund, P. (2006) Thermofluor-based high-throughput stability optimization of proteins for structural studies. *Anal. Biochem.* **357**, 289–298
19. Cornish-Bowden, A. (1999) *Fundamentals of Enzyme Kinetics*. Portland Press Ltd, London
20. Coulter, C.V., Gerrard, J.A., Kraunsoe, J.A.E., and Pratt, A.J. (1996) *(S)*-Aspartate semi-aldehyde: synthetic and structural studies. *Tetrahedron* **52**, 7127–7136
21. Robinson-Rechavi, M., Alibes, A., and Godzik, A. (2006) Contribution of electrostatic interactions, compactness and quaternary structure to protein thermostability: lessons from structural genomics of *Thermotoga maritima*. *J. Mol. Biol.* **356**, 547–557
22. Robinson-Rechavi, M. and Godzik, A. (2005) Structural genomics of *Thermotoga maritima* proteins shows that contact order is a major determinant of protein thermostability. *Structure* **13**, 857–860
23. Walden, H., Bell, G.S., Russell, R.J.M., Siebers, B., Hensel, R., and Taylor, G.L. (2001) Tiny TIM: a small, tetrameric, hyperthermostable triosephosphate isomerase. *J. Mol. Biol.* **306**, 745–757
24. Matulis, D., Kranz, J.K., Salemme, F.R., and Todd, M.J. (2005) Thermodynamic stability of carbonic anhydrase: measurements of binding affinity and stoichiometry using ThermoFluor. *Biochemistry* **44**, 5258–5266
25. Daniel, R.M. (1996) The upper limits of enzyme thermal stability. *Enzyme Microb. Tech.* **19**, 74–79
26. Wrba, A., Schweiger, A., Schultes, V., Jaenicke, R., and Zavodszky, P. (1990) Extremely thermostable D-glyceraldehyde-3-phosphate dehydrogenase from the eubacterium *Thermotoga maritima*. *Biochemistry* **29**, 7584–7592
27. Varley, P.G. and Pain, R.H. (1991) Relation between stability, dynamics and enzyme-activity in 3-phosphoglycerate kinases from yeast and *Thermus thermophilus*. *J. Mol. Biol.* **220**, 531–538
28. Huber, R., Langworthy, T.A., Konig, H., Thomm, M., Woese, C.R., Sleytr, U.B., and Stetter, K.O. (1986) *Thermotoga maritima sp* represents a new genus of unique extremely thermophilic eubacteria growing up to 90 degrees C. *Arch. Microbiol.* **144**, 324–333
29. Rodionov, D.A., Vitreschak, A.G., Mironov, A.A., and Gelfand, M.S. (2003) Regulation of lysine biosynthesis and transport genes in bacteria: yet another RNA riboswitch? *Nucleic Acids Res.* **31**, 6748–6757
30. DeLano, W.L. (2002) *The PyMOL Molecular Graphics System*. DeLano Scientific, San Carlos, CA, USA. http://www.pymol.org